Correspondence

Throughput Maximization for a Buffer-Aided Successive Relaying Network Employing Energy Harvesting

Shruti Gupta, Rong Zhang, and Lajos Hanzo

***Abstract*—Energy harvesting (EH)-assisted nodes are capable of significantly prolonging the lifetime of future wireless networks, provided that they rely on appropriate transmission policies, which accommodate the associated stochastic energy arrival. In this paper, a successive-relaying-based network using rechargeable source and relay nodes having limited buffers for both their energy and data storage is considered. The maximization of the network throughput with noncausal knowledge of energy arrivals by the deadline T is formulated as a nonconvex optimization problem, and it is solved using the interior-point optimization (IPOPT) method. The performance of the low-complexity suboptimal scheme was found to reach its maximum when the two phases of the successive relaying protocol have equal duration. The optimal and suboptimal schemes are capable of achieving up to 92% and 88% of the throughput performance of the benchmark scheme. The suboptimal scheme's throughput performance is consistently about 90% of that of the optimal scheme. For asymmetric data (or energy) buffer sizes, it was found that the throughput performance depends on the total (i.e., collective) data (or energy) buffer capacity available in the network and not just on the smallest data buffer.**

***Index Terms*—Author, please supply index terms/keywords for your paper. To download the IEEE Taxonomy go to http://www.ieee.org/documents/taxonomy_v101.pdf.** AQ1

I. Introduction

Cooperative communication is capable of attaining significant throughput and reliability improvements, where the source node (SN) and cooperating relay nodes (RN) expend their energy while processing and transmitting the signal to the destination node (DN). The nodes are typically powered through precharged batteries, but once these batteries are drained, the nodes become dysfunctional [1], [2]. An emerging solution to this vexed problem is the use of energy harvesting (EH) [1]–[3], which has to be capable of accommodating the random arrivals of energy and its storage at the nodes [4].

Hence, EH communication systems have been studied under different network models. In [5]–[7], a single-user EH system was characterized, where beneficial power-allocation strategies were designed under the corresponding EH constraints. This was further extended to the design of an EH-aided broadcast channel in [8] and [9] and to two-way orthogonal frequency-division multiplexing communications [10]. In [8], Yang *et al.* defined the *cutoff power* levels for each user to allocate the optimal power to them, whereas in [9], Kuan *et al.* analyzed the tradeoff between the achievable reliability and throughput for broadcast transmissions relying on erasure codes for EH sensors. In [10], the receiver is designed both for simultaneously processing information and for harvesting energy from the received desired signal, as well as jamming interference a through power splitter. In recent years, cooperative networks have also been studied in the context of EH at the RNs and/or the SN [1]–[3], [11]–[13]. Specifically, in [1], Medepally and Mehta investigated the benefits of relay selection relying on multiple EH amplify-and-forward RNs, whenever they have sufficient energy for transmission. By contrast, in [2], information-buffer-aided link activation was used, which was controlled both by the quality of the links and by the amount of energy buffered at these nodes. Two-hop networks relying either on a single or on a pair of parallel RNs using a successive relaying protocol were investigated to quantify the benefits of both multiple relays and of EH on the average throughput of the system in [3]. In [11], the authors derived the optimal achievable rates for an EH system in the context of two-way relaying employing different relaying strategies. Furthermore, a similar two-way EH relay system employing time-division broadcasting and multiple access broadcasting, which was subjected to channel state uncertainty, was considered in the context of joint energy and transmit time allocation in [12]. Utilizing the structure of a specific problem and the generalized optimality principle, in [13], a new algorithm for constrained utility maximization problems encountered in a cooperative network of wireless sensor nodes is formulated.

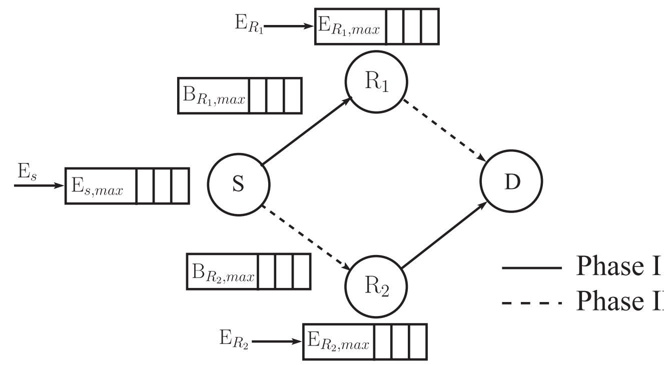

Fig. 1. Successive relaying network where EH nodes are equipped with finite buffer for both energy and data storage.

Against this background, we consider a successive relaying model, which is capable of mimicking a full-duplex (FD) RN, despite relying on a pair of half-duplex (HD) RNs, which are activated alternately in their transmitter and receiver modes to create a virtual FD relay. This HD regime reduces the complexity of the FD system, since the FD RN would require high-complexity interference cancellation at the receiver. In contrast to [3], our model relies on the realistic constraint that EH nodes (SN, RN_1, RN_2) have a finite energy storage capacity and that the RNs also have limited data buffers for storing the source data. We first formulate an optimization problem for the throughput maximization of our successive-relaying-aided network in Fig. 1 having finite buffers, as well as relying on the idealized noncausal knowledge of the energy arrivals at all EH nodes. Then, using the interior-point optimization method (IPOPT), the optimization problem is solved for both optimal and suboptimal schemes, and finally, we quantify the effect of buffer sizes on the throughput of the network based on both schemes. While proof-of-concept studies are indeed

Manuscript received January 28, 2015; revised June 3, 2015 and July 30, 2015; accepted September 8, 2015. This work was supported by the European Research Council under the Advanced Fellow Grant. The review of this paper was coordinated by Dr. L. Zhao.

The authors are with the School of Electronics and Computer Science, University of Southampton, Southampton SO17 1BJ, U.K. (e-mail: sg7g12@ecs.soton.ac.uk; rz@ecs.soton.ac.uk; lh@ecs.soton.ac.uk).

Color versions of one or more of the figures in this paper are available online at http://ieeexplore.ieee.org.

Digital Object Identifier 10.1109/TVT.2015.2477808

valuable, the ultimate purpose of most engineering studies is to attempt a real-world implementation of the proposed techniques. Through this study, we aimed to take the valuable proposals in [3] a step closer to its real-world deployment. Explicitly, the novelty of this contribution is given as follows: 1) We define a practical successive relaying model constrained by both limited energy and data storage buffers at the EH nodes, which dispenses with the idealized simplifying assumption of having infinite buffers [3]; 2) we formulate the optimal transmission policy; and 3) we propose a suboptimal transmission scheme capable of approaching the performance of its optimal counterpart at significantly reduced complexity, which is achieved at the expense of a marginally degraded performance. In our study, we also consider the scenario of asymmetric fading, energy, and data buffers. This paper is organized as follows. In Section II, our system model is presented, which is followed by the formulation of our optimization problem in Section III. Our results are discussed in Section IV, whereas our conclusions are offered in Section V.

II. System Model

We consider the successive relaying technique of [3] having two phases, where the RNs assist the SN's transmission to the DN, as shown in Fig. 1. In Phase I in Fig. 1, the SN transmits to RN_1, whereas RN_2 simultaneously transmits to the DN. By contrast, in Phase II in Fig. 1, SN and RN_1 transmit simultaneously both to RN_2 and to DN, respectively. Thus, the SN is always transmitting, whereas the DN is always receiving during the process. It is assumed that there is no direct link between $SN{-}DN$ and $RN_1{-}RN_2$, as well as that these are decode-and-forward (DF) HD RNs that are located sufficiently far apart from each other to avoid any interference. We assume that SN, RN_1, and RN_2 harvest energy from the environment and have finite energy buffers that can store a maximum of $E_{S,\max}$, $E_{R1,\max}$, and $E_{R2,\max}$ units, respectively, whereas RN_1 and RN_2 are also equipped with data buffers of $B_{R1,\max}$ and $B_{R2,\max}$ packets, respectively. For ease of exposition, we merge the energy arrival events at all the EH nodes into a single time series $(t_0, t_1, \ldots, t_K)$ by considering zero amount of energy arrivals at the nodes that do not harvest energy at some instant t_k. More explicitly, the EH processes at the EH nodes are independent of each other. In other words, the energy arrival instances of a node may be different from those of the other nodes. For example, assume that an energy arrival occurred at node RN_1 at some instant t_k, whereas there was no energy arrival at the other nodes (S and RN_2) at the time instant t_k. In our mathematical analysis, we assumed that at time instant t_k, nodes S and RN_2 harvested zero amount of energy. We set $t_0 = 0$ and $t_K = T$. We represent the amount of energy harvested at SN, RN_1, and RN_2 at time instant t_k as $E_{S,k}$, $E_{R1,k}$, and $E_{R2,k}$ units, respectively, for $k = 0, 1, \ldots K-1$. The time interval between the two consecutive energy arrivals is termed as an *epoch*, whose length is defined as $\tau_k = t_k - t_{k-1}$. The complex-valued channel gains are considered to be constant throughout the communication process preceding the deadline. The channel gain between the nodes L and M is denoted by H_{LM}, where we have $L \in \{SN, R_1N, R_2N\}$ and $M \in \{RN_1, RN_2, DN\}$.

We consider the throughput maximization problem under the idealized simplifying assumption of having prior knowledge about the energy arrivals at all the EH nodes before the commencement of the communication process. We assume that the energy expended at the nodes is only the transmission energy and that perfect "capacity-achieving" codes are used, which facilitate operation exactly at the Shannon capacity, thus determining the rate versus power relationship of a given link, which is given by

$$r\left[p(t)\right] = \log_2\left[1 + Hp(t)\right] \tag{1}$$

where H is the channel gain of the link, and $p(t)$ is the transmission power of the node at time t. As a result of energy arrivals over time and as a benefit of the energy storage capacity at the nodes, any feasible transmission policy should satisfy following constraints.

1) Energy causality constraint: The total energy expended by a node during its transmission session should not exceed the total energy harvested by that node until that time.
2) Energy overflow constraint: The energy exceeding the storage capacity of the energy buffer at the node is lost owing to overflow.
3) Data causality constraint: The total data transmitted by a node during the process should not exceed the total data received by that node until that time.
4) Data overflow constraint: The amount of data exceeding the storage capacity of data buffer is lost due to overflow.

III. Problem Formulation

Here, we first stipulate some properties of the optimal transmission policy in the following two lemmas, which will be used to formulate the throughput maximization problem for the system in Fig. 1. The proof of these lemmas is provided in Appendixes A and B.

Lemma 1: The transmission rate/power of a node is constant between two consecutive energy arrivals but potentially changes when new energy arrives at the node [3].

Lemma 2: The feasible transmission policy ensures that the relays are always on without decreasing the throughput of the system [3].

Based on Lemmas 1 and 2, we can characterize the optimal policy in the following way. There is a constant transmission rate for the pair of nodes between consecutive energy arrivals according to the optimal policy, as formulated in Lemma 1. Therefore, we assume that the transmission power of SN during Phases I and II in Fig. 1 in an epoch is constant and given by $p_{SI,k}$ and $p_{SII,k}$, respectively. Similarly, the transmission power of RN_1 and RN_2 is denoted by $p_{R_1,k}$ and $p_{R_2,k}$, respectively. Lemma 2 implies that we restrict our attention to the specific transmission policies, where both RN_1 and RN_2 are always on for the sake of defining a feasible transmission policy. Thus, we assume that the total transmission time between $SN{-}RN_1$ and $RN_2{-}DN$ is the same and denote this duration of Phase I between the time instants t_{k-1} and t_k by $L_{I,k}$. Similarly, we assume the same transmission time between $SN{-}RN_2$ and $RN_1{-}DN$ in Phase II, which is denoted by $L_{II,k}$, $k = 1, 2, \ldots, K$. Finally, we identify the optimal transmission policy that defines which particular node transmits and when, along with the specific power allocation of each node. We then define a suboptimal scheme, where the duration of each phase of successive relaying is fixed to a particular ratio.

A. Optimal Transmission Policy

Let us now define the optimization problem of maximizing the system throughput by the deadline T. Since RN_2 initially has no data in Phase I in Fig. 1, it is assumed without loss of generality that it starts transmission by delivering $\epsilon > 0$ amount of dummy information to DN, where ϵ is sufficiently small to be ignored for our throughput optimization problem. Upon scheduling the two phases in succession, it is ensured that there is no further throughput loss for the system. In other words, at the beginning of transmission, RN_2 possesses no data from S that can be transmitted to DN; hence, it commences its transmission with ϵ dummy packets. However, subsequently, the transmission phases occur in immediate succession without any interval. This ensures that there is no need to send dummy packets, and thus, no further loss of system throughput is imposed. Similar assumptions were also made in [3]. We first define the throughput of the nodes in different phases based on the rate versus power relationship (1) mentioned in Section II as

$$\begin{aligned}\alpha_{R1,k} &= L_{II,k}\log_2(1+H_{R1D}p_{R1,k})\\ \alpha_{R2,k} &= L_{I,k}\log_2(1+H_{R2D}p_{R2,k}) \qquad (2a)\\ \alpha_{SI,k} &= L_{I,k}\log_2(1+H_{SR1}p_{SI,k})\\ \alpha_{SII,k} &= L_{II,k}\log_2(1+H_{SR2}p_{SII,k}). \qquad (2b)\end{aligned}$$

Now, the optimization problem is defined over $L_{I,k}$, $L_{II,k}$, $\alpha_{SI,k}$, $\alpha_{SII,k}$, $\alpha_{R1,k}$, and $\alpha_{R2,k}$, (3a)–(3m), shown at the bottom of the page.

Note that when (3h)–(3i) are evaluated at $k = K$, the total amount of data delivered to DN is equal to the amount of data transferred by RN_1 and RN_2; hence, the throughput maximization problem corresponds to the maximization of the amount of data transmitted by both the RNs, as formulated in (3a). The problem in (3) is a nonconvex optimization problem, owing to the nonconvex energy storage constraints defined in (3e)–(3g), which can be efficiently solved using the IPOPT method, as given in Appendix C.

B. Suboptimal (Alternate) Transmission Policy

In this scheme, we set the duration of Phase I in Fig. 1 to be equal to η%; of the length of an epoch, i.e., we have

$$L_{I,k} = \frac{\eta}{100}\tau_k, \quad L_{II,k} = \tau_k - \frac{\eta}{100}\tau_k. \qquad (4)$$

$$\text{maximize} \quad \sum_{k=1}^{K}\alpha_{R1,k}+\alpha_{R2,k} \qquad (3a)$$

subject to

Energy causality constraints (constraint 1 in Section II) at $SN,\ RN_1,$ and RN_2:

$$\sum_{j=1}^{k}\frac{L_{I,j}}{H_{SR1}}\left(2^{\left(\frac{\alpha_{SI,j}}{L_{I,j}}\right)}-1\right)+\frac{L_{II,j}}{H_{SR2}}\left(2^{\left(\frac{\alpha_{SII,j}}{L_{II,j}}\right)}-1\right)\le\sum_{j=0}^{k-1}E_{S,j} \qquad \forall\, k \qquad (3b)$$

$$\sum_{j=1}^{k}\frac{L_{II,j}}{H_{R1D}}\left(2^{\left(\frac{\alpha_{R1,j}}{L_{II,j}}\right)}-1\right)\le\sum_{j=0}^{k-1}E_{R1,j} \qquad \forall\, k \qquad (3c)$$

$$\sum_{j=1}^{k}\frac{L_{I,j}}{H_{R2D}}\left(2^{\left(\frac{\alpha_{R2,j}}{L_{I,j}}\right)}-1\right)\le\sum_{j=0}^{k-1}E_{R2,j} \qquad \forall\, k. \qquad (3d)$$

Energy overflow constraints (constraint 2 in Section II) at $SN,\ RN_1,$ and RN_2:

$$\sum_{j=0}^{k}E_{S,j}-\sum_{j=1}^{k}\frac{L_{I,j}}{H_{SR1}}\left(2^{\left(\frac{\alpha_{SI,j}}{L_{I,j}}\right)}-1\right)+\frac{L_{II,j}}{H_{SR2}}\left(2^{\left(\frac{\alpha_{SII,j}}{L_{II,j}}\right)}-1\right)\le E_{S,\max} \qquad \forall\, k \qquad (3e)$$

$$\sum_{j=0}^{k}E_{R1,j}-\sum_{j=1}^{k}\frac{L_{II,j}}{H_{R1D}}\left(2^{\left(\frac{\alpha_{R1,j}}{L_{II,j}}\right)}-1\right)\le E_{R1,\max} \qquad \forall\, k \qquad (3f)$$

$$\sum_{j=0}^{k}E_{R2,j}-\sum_{j=1}^{k}\frac{L_{I,j}}{H_{R2D}}\left(2^{\left(\frac{\alpha_{R2,j}}{L_{I,j}}\right)^{i}}-1\right)\le E_{R2,\max} \qquad \forall\, k. \qquad (3g)$$

Data causality constraints (constraint 3 in Section II) at RN_1 and RN_2:

$$\sum_{j=1}^{k}\alpha_{R1,j}\le\sum_{j=1}^{k}\alpha_{SI,j} \qquad \forall\, k \qquad (3h)$$

$$\sum_{j=1}^{k}\alpha_{R2,j}\le\sum_{j=1}^{k}\alpha_{SII,j} \qquad \forall\, k. \qquad (3i)$$

Data overflow constraints (constraint 4 in Section II) at RN_1 and RN_2:

$$\sum_{j=1}^{k}\alpha_{SI,j}-\sum_{j=1}^{k-1}\alpha_{R1,j}\le B_{R1,\max} \qquad \forall\, k \qquad (3j)$$

$$\sum_{j=1}^{k}\alpha_{SII,j}-\sum_{j=1}^{k-1}\alpha_{R2,j}\le B_{R2,\max} \qquad \forall\, k. \qquad (3k)$$

Half duplex constraint due to the HD relays RN_1 and RN_2:

$$L_{I,k}+L_{II,k}\le\tau_k \qquad \forall\, k. \qquad (3l)$$

Feasibility constraints at $SN,\ RN_1$ and RN_2:

$$\alpha_{SI,k}\ge 0,\quad \alpha_{SII,k}\ge 0,\quad \alpha_{R1,k}\ge 0;\alpha_{R2,k}\ge 0,\quad L_{I,k}\ge 0,\quad L_{II,k}\ge 0 \qquad \forall\, k \qquad (3m)$$

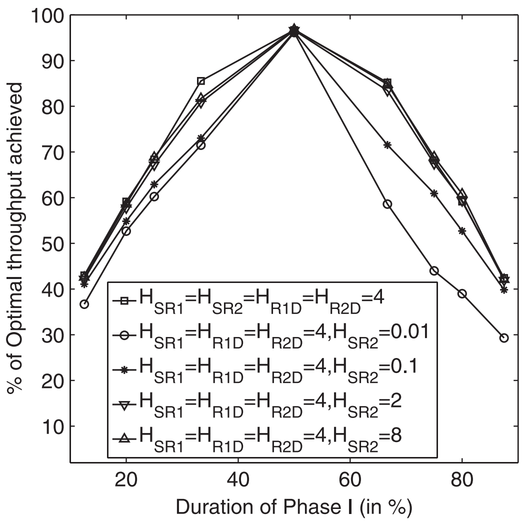

Fig. 2. Relation between percentage of optimal throughput achieved for varying duration of Phase I occurring in an EH epoch with sufficient energy and data buffer sizes (5 and 2, respectively) for different settings of channel gains.

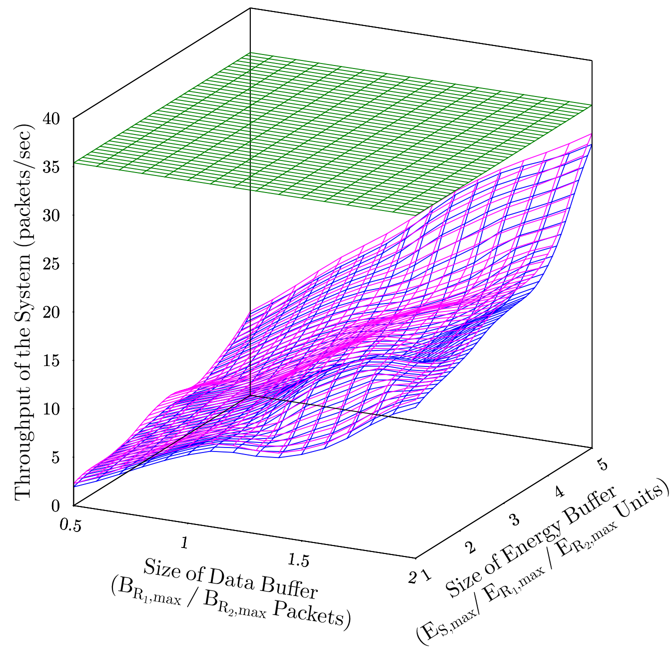

Fig. 3. Impact of the energy and data buffer sizes at all the EH nodes on the throughput of the system by the deadline T. The constant green surface represents the throughput of the benchmark scheme [3], whereas the pink and blue surfaces depict our optimal and suboptimal transmission policies, respectively.

Using (4), the optimization problem is relaxed for this suboptimal scheme and can be reformulated by omitting (3l) from (3). This is again a nonconvex optimization problem; hence, it may be solved using the IPOPT method. This scheme is termed suboptimal, since the duration of the phases has been deliberately fixed for the sake of reducing the complexity[1] of the optimization problem.

IV. Performance Results

Here, we evaluate the performance of the proposed buffer-aided successive relaying system relying on offline power allocation in terms of the optimal throughput achieved by the deadline of $T = 10\,\text{s}$. We assume that the EH process of both the SN and the RNs independently takes values from $[0, E_{\max} = 5]$ units, where the energy is uniformly distributed under an exponential inter-arrival time at a rate of $\lambda_e = 5\,\text{units/s}$. The deterministic channel gains are set to the values $H_{SR1} = H_{SR2} = H_{R1D} = H_{R2D} = 4$, except otherwise mentioned. Our results quantify the throughput of the system as a function of both data and energy buffer capacity for both optimal and suboptimal schemes that are benchmarked against the infinite-storage-based optimal scheme defined in [3]. Our benchmark scheme of [3] is insensitive to the buffer sizes, since it considers infinite storage capacities at all the EH nodes for both energy and data, thereby providing an upper bound to our proposed system.

The percentage duration of Phases I and II in Fig. 1 is not fixed for the optimal scheme, whereas they have been fixed to a specific ratio for the suboptimal scheme for the sake of complexity reduction. Hence, our first goal was to identify the specific ratio of the durations of Phases I and II that would maximize the throughput of the suboptimal scheme. Fig. 2 shows the specific percentage of the optimal throughput, which was actually achieved by varying the proportion of the Phase I duration (L_I) in each of the EH epochs, along with the symmetric $(H_{SR1} = H_{SR2} = H_{R1D} = H_{R2D} = 4)$ and asymmetric settings of the channel fading gain for $SN{-}RN_2$. The performance of the suboptimal scheme peaks when the durations of both phases are equal. For the other scenarios, the throughput is lower, because the amount of data transmitted between SN and DN is limited by the shorter phase. It is shown in Fig. 2 that, as the duration of the shorter phase increases, the throughput also increases. It is interesting to note that in the scenarios of very low channel gain, i.e., for $H_{SR2} = 0.01$ and $H_{SR2} = 0.1$, there exists asymmetry in the throughput achieved by the system. The reason behind this trend is that when the duration of Phase I is higher than that of Phase II, the channel gain of path $SN{-}RN_2$ limits the amount of data that can be otherwise transmitted to RN_2. As shown in Fig. 2, when the duration of Phase I is 50% of the EH epoch, the suboptimal scheme achieves approximately 97% of the optimal scheme's throughput. Hence, in the following discussions, we consider a suboptimal scheme, where the duration of each phase is 50% of the epoch duration.

The 3-D characterization of the system in Fig. 1 is provided in Fig. 3. Specifically, Fig. 3 shows the overall throughput of the system as a function of the size of both energy and data buffers at the EH nodes. It can be clearly observed that, with the increase in the size of buffers at the EH nodes, the throughput of our proposed schemes improve owing to increased availability of energy and data storage capacity at the EH nodes, supporting a larger amount of data transmission to DN. However, the throughput of the benchmark scheme [3] is constant, i.e., independent of the buffer sizes, as it relies on the idealized settings where EH nodes possess infinite energy and data storage capacity. Moreover, our optimal scheme performs only marginally better than our less complex suboptimal scheme, because the duration of each phase is fixed in the suboptimal scheme. This would, in turn, result in limiting the amount of data that can be transmitted to DN during successive relaying phases. To closely analyze the impact of the energy and data buffer capacities at the EH nodes on the overall system throughput, we present the 2-D curves corresponding to the individual analysis of the energy buffer size while keeping the data buffer size constant, and *vice versa*.

The results in Fig. 4 show the throughput of the system against the size of the battery in the presence of sufficient, insufficient, and asymmetric data buffer sizes for both optimal and suboptimal schemes. As expected, upon increasing the battery size, the throughput of the system is improved, owing to the availability of increased amount of

[1]The complexity analysis of both schemes is beyond the scope of this paper.

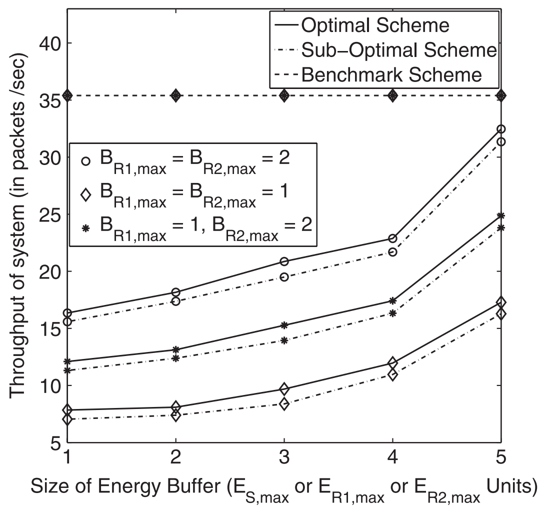

Fig. 4. Impact of energy buffer size at all the EH nodes with sufficient (two packets), insufficient (one packet), and asymmetric data buffer capacity at the RNs on the throughput of the system by the deadline T.

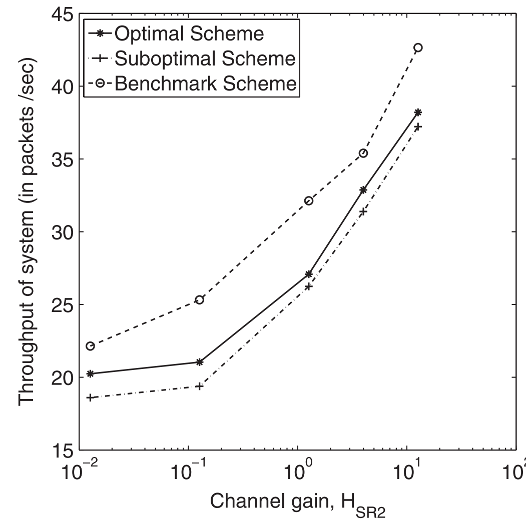

Fig. 6. Impact of asymmetric fading from S to RN_2 for sufficient battery and data buffer capacities (five units and two packets, respectively) at EH nodes on throughput of the system by the deadline T.

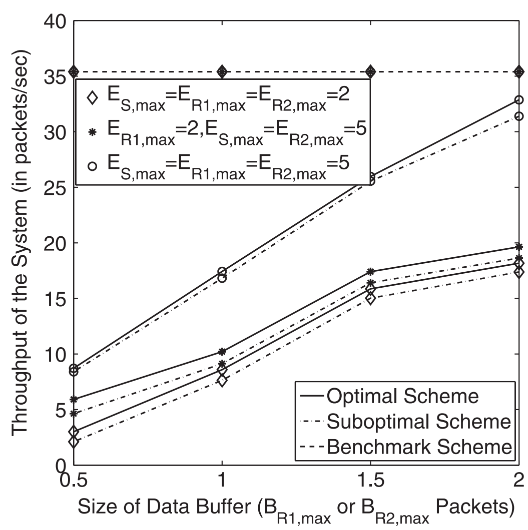

Fig. 5. Impact of data buffer size at the RNs with sufficient (five units), insufficient (two units), and asymmetric battery capacities at EH nodes over throughput of the system by the deadline T.

energy (due to the increase in buffer size) for transmission. Moreover, it can be observed that for sufficient (or insufficient) data storage, our optimal system is capable of achieving 92% (or 50%) of the benchmark scheme's throughput performance [3], whereas our suboptimal scheme performs slightly worse than the optimal scheme, reaching 88% (or 46%) of the benchmark system's throughput value in [3], when the battery capacity of the EH nodes is sufficiently high ($E_{S,\max} = E_{R_1,\max} = E_{R_2,\max} = 5\,\text{units}$). Furthermore, for asymmetric settings having unequal data buffers at RN_1 and RN_2, the throughput becomes lower than that for sufficiently large storage, since RN_1 is now acting as a bottleneck, preventing the flow of data to DN. On the other hand, for this asymmetric setting, the throughput becomes higher than that for insufficient storage, since the node RN_2 has a higher data storage capacity, thereby supporting a higher data rate to DN. The suboptimal scheme's throughput performance was 95.2%, 90.7%, and 93.7% of that of the optimal scheme for the scenarios of sufficient, insufficient, and asymmetric data buffers, respectively.

Similarly, Fig. 5 shows the throughput of the system as a function of the data buffer size at the RNs with sufficient, insufficient, and asymmetric energy buffer sizes for both optimal and suboptimal schemes. It is clearly demonstrated that as the size of the data buffer increases, the amount of data successfully transmitted to the DN also increases for both schemes, indicating that the optimal and suboptimal schemes have quite similar performance. The reason behind this trend is the reduction of overflowing data buffers owing to the larger capacities of these buffers at the RNs. Furthermore, for sufficient (or insufficient) battery capacities, our optimal system having finite buffers is capable of achieving 92% (or 52%) of the throughput compared with our suboptimal scheme that performs comparably, since it achieves 88% (or 49%) of the benchmark system's throughput [3] for the maximum data buffer size of $B_{R_1,\max} = B_{R_2,\max} = 2\,\text{packets}$. Furthermore, for asymmetric settings having unequal energy buffers at RN_1 and RN_2, the throughput becomes lower than that for a sufficiently large storage, since RN_1 is low on energy, hence preventing the flow of data to DN. On the other hand, for this asymmetric setting, the throughput becomes higher than that for insufficient storage, since the node RN_2 has a higher energy storage capacity, consequently supporting a higher data rate to DN. Moreover, the suboptimal scheme achieves 96.7%, 87.3%, and 94.2% of the throughput of our optimal scheme for sufficient, insufficient, and asymmetric energy buffers, respectively.

Fig. 6 shows the throughput of the system as a function of the asymmetric channel gain of the $SN{-}RN_2$ path (H_{SR2}) for the scenario of having a sufficiently high data and energy buffer size at the EH nodes, where all other channel gains are set to $H_{SR1} = H_{R1D} = H_{R2D} = 4$. It can be clearly seen that as the channel gain H_{SR2} increases, the throughput of the system increases for all the schemes owing to the rate–power relationship mentioned in (1). This means that as the value of the channel gain increases, the amount of data transmitted from SN to RN_2 increases, and so does the amount of data reaching the DN, hence, also increasing the overall throughput of the system. As expected, the benchmark scheme represents the upper bound of the system's throughput for an asymmetric setting of the channel gain, as it relies on the idealized assumptions of infinite data and energy storage capacities at the EH nodes. However, our optimal scheme performs better than the suboptimal scheme owing to the fixed duration of phases in the successive relaying protocol of the latter scheme.

In Fig. 7, we considered the throughput of the system as a function of the data buffer capacity at the RNs for the scenario of asymmetric channel gains and asymmetric energy buffer capacity. Explicitly, we

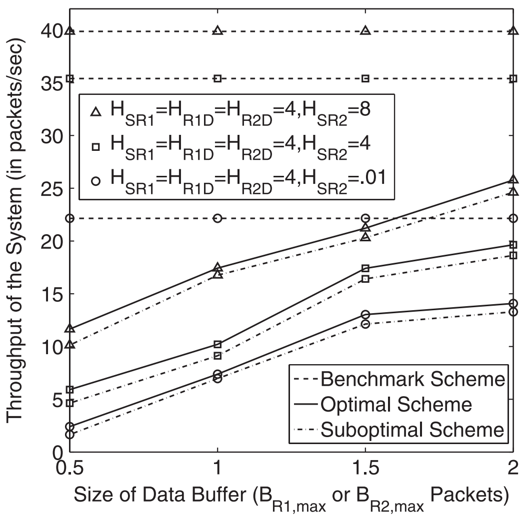

Fig. 7. Impact of data buffer size at the RNs with asymmetric channel gains and battery capacities ($E_{S,\max} = E_{R2,\max} = 5$ units, and $E_{R1,\max} = 2$ units) at EH nodes over throughput of the system by the deadline T.

have used $E_{S,\max} = E_{R2,\max} = 5$ units and $E_{R1,\max} = 2$ units at the EH nodes. The benchmark scheme provides an upper bound for our proposed schemes and has a constant throughput, since it is unaffected by the data and energy buffer capacity at the EH nodes. Interestingly, the throughput of the system improves upon increasing the value of the channel gains, which becomes explicit by observing the rate–power relationship of (1). Moreover, the asymmetric setting of energy buffers at the EH nodes of the proposed scheme results in limiting the throughput achieved by the system, because RN_1 is acting as the bottleneck owing to the low energy buffer capacity.

In light of the preceding study, our findings for the realistic simulation parameters in Table I may be summarized as follows.

1) The performance of the suboptimal scheme as a percentage of the throughput achieved by the optimal scheme reaches its maximum when the two phases of the successive relaying protocol have equal duration.
2) The optimal and suboptimal schemes are capable of achieving up to 92% and 88% of the benchmark scheme's throughput [3] for sufficiently high energy and data buffer capacities.
3) The suboptimal scheme's throughput is consistently about 90% of that of the optimal scheme.
4) For asymmetric data (or energy) buffer sizes, the attainable throughput depends on the total (i.e., collective) data (or energy) buffer capacity available in the network and not only on the smallest data buffer.

V. Conclusion

In this paper, we have considered the throughput optimization of an EH-assisted two-hop network using a buffer-aided successive relaying protocol. Under the assumption of known energy arrivals, we defined the related nonconvex optimization problem and proposed both optimal and suboptimal schemes to maximize the data delivered to the DN by the deadline. Then, using the *interior-point* method, an efficient solution was found for both schemes. Finally, our results justify that both our optimal and suboptimal schemes are capable of performing close to the benchmark system [3]. Furthermore, the less-complex suboptimal scheme is capable of approaching the performance of our optimal scheme at the expense of a slight performance degradation, provided that the EH nodes are equipped with sufficiently large buffers for both energy and data storage. Our future work may consider EH-aided adaptive transceiver schemes.

Appendix A
Proof of Lemma 1

This proof is an extension of that derived for the point-to-point case in [5] to the two-hop scenario defined in this paper. Let us assume that the transmitter nodes (SN, RN_1, RN_2) change their transmission rate between two EH instances t_i and t_{i+1}. Let us furthermore denote the rates by $r_{M,n}$ and $r_{M,n+1}$ and the instant when the rate changes by t'_i, where we have $M \in \{SI, R2\}$ in Phase I and $M \in \{SII, R1\}$ in Phase II of the successive relaying protocol. Correspondingly, the duration of each phase can be written as $L_{I,n}$, $L_{I,n+1}$, $L_{II,n}$, and $L_{II,n+1}$. Let us now consider the duration $[t_i, t_{i+1})$. The total energy consumed in this duration at SN is $p_{SI,n}L_{I,n} + p_{SII,n}L_{II,n} + p_{SI,n+1}L_{I,n+1} + p_{SII,n+1}L_{II,n+1}$. Similarly, the total energy consumed at RN_1 is $p_{R1,n}L_{II,n} + p_{R1,n+1}L_{II,n+1}$ and that at RN_2 is $p_{R2,n}L_{I,n} + p_{R2,n+1}L_{I,n+1}$. Let us now consider SN in more detail and define

$$p'_{SI} = \frac{p_{SI,n}L_{I,n} + p_{SI,n+1}L_{I,n+1}}{t_{i+1} - t_i}$$

$$p'_{SII} = \frac{p_{SII,n}L_{II,n} + p_{SII,n+1}L_{II,n+1}}{t_{i+1} - t_i}$$

$$r'_{SI} = r\left[p'_{SI}\right] = r\left[\frac{p_{SI,n}L_{I,n} + p_{SI,n+1}L_{I,n+1}}{t_{i+1} - t_i}\right]$$

$$r'_{SII} = r\left[p'_{SII}\right] = r\left[\frac{p_{SII,n}L_{II,n} + p_{SII,n+1}L_{II,n+1}}{t_{i+1} - t_i}\right].$$

Let us now use these r'_{SI} and r'_{SII} as the new transmission rates for Phases I and II at SN over $[t_i, t_{i+1})$ and keep the rest of the rates the same as in the original policy. It is easy to observe that the new transmission policy is feasible, since all the energy constraints are satisfied under this policy. On the other hand, we can write the total number of packets that are departed from SN in both of the phases over this duration under this new policy as

$$\begin{aligned}(r'_{SI} + r'_{SII})(t_{i+1} - t_i) &= (r\left[p'_{SI}\right] + r[p'_{SII}])(t_{i+1} - t_i)\\ &= \left(r\left[\frac{p_{SI,n}L_{I,n} + p_{SI,n+1}L_{I,n+1}}{t_{i+1} - t_i}\right]\right)(t_{i+1} - t_i)\\ &\quad + \left(r\left[\frac{p_{SII,n}L_{II,n} + p_{SII,n+1}L_{II,n+1}}{t_{i+1} - t_i}\right]\right)(t_{i+1} - t_i) \qquad \text{(5a)}\\ &\geq (r[p_{SI,n}]L_{I,n} + r[p_{SI,n+1}]L_{I,n+1})\\ &\quad + (r[p_{SII,n}]L_{II,n} + r[p_{SII,n+1}]L_{II,n+1}) \qquad \text{(5b)}\\ &= r_{SI,n}L_{I,n} + r_{SI,n+1}L_{I,n+1} + r_{SII,n}L_{II,n}\\ &\quad + r_{SII,n+1}L_{II,n+1} \qquad \text{(5c)}\end{aligned}$$

where the inequality in (5b) follows from (1) in Section II, which is a concave function of the transmission power p. Therefore, the total number of packets transmitted by SN in this duration under the new policy is higher than those that are departed under the original policy. Similarly, we can prove that the RNs under this new policy will send more data to DN. If we keep all the rates constant, the transmissions will deliver larger amounts of data to DN by the deadline. This contradicts the optimality of the original transmission policy.

APPENDIX B
PROOF OF LEMMA 2

The proof derived for the two-relay case extends the single-relay case of [14]. In the case of two parallel relays, we consider a feasible transmission policy where one of the relays (e.g., RN_1) is not always on, i.e., it is not transmitting or receiving data all the time. Now, if we have an idle time interval right at the beginning of Phase I, we can extend the epoch of SN in Phase II, ensuring that there is no idle time. Note that this strategy continues to satisfy all the causality and storage constraints. On the other hand, if an idle time duration occurs at the beginning of Phase II, we can delay the epoch of relay RN_1 without violating the feasibility of our policy, because it can store more energy in the meantime, and the previous argument can be used to extend the epoch of RN_2 during Phase I to avoid any idle time. Similarly, we can consider the scenario when RN_2 is not always on. Therefore, we remove the idle times by increasing the transmission duration of one of the nodes (SN or RNs) while keeping the total amount of transmitted data the same. Since the rate–power relation of (1) is concave, the new policy conveys the same amount of data to DN while consuming less energy. Hence, it is feasible. Moreover, using this proof, we can say that there exists an optimal policy, where SN and DN are always on for the twin-relay system relying on a successive relaying protocol.

APPENDIX C
INTERIOR-POINT OPTIMIZATION METHOD

The relevant optimization techniques include IPOPT, LOQO, and KNITRO [15]. The IPOPT method is more efficient than the other two techniques, because it relies on tighter termination bounds and utilizes comparable CPU time to evaluate a higher number of objective function values and iterations [15]. The IPOPT method involves the primal–dual interior-point algorithm with the aid of a so-called filter line-search method invoked for nonlinear programming [15], [16], which improves its robustness over that of LOQO and KNITRO. In the primal–dual interior-point method, both primal and dual variables are updated, whereas primal and dual iterates do not have to be feasible. The search direction in this method is obtained using Newton's method applied to the modified Karush–Kuhn–Tucker equations. However, the basic idea behind the filter line-search algorithm involves considering a trial point during the backtracking line search, where this trial point is considered to be acceptable if it leads to sufficient progress toward achieving the optimization goal. This algorithm maintains a "filter," which is a set of values that both the objective function and the constraint violation functions are prohibited from returning. For a trial point to be successful, the values of the objective function and the constraint violation functions evaluated at that trial point should not be a member of the filter. This filter is updated at every iteration to ensure that the algorithm does not cycle in the neighborhood of the previous iterate [15].

REFERENCES

[1] B. Medepally and N. Mehta, "Voluntary energy harvesting relays and selection in cooperative wireless networks," *IEEE Trans. Wireless Commun.*, vol. 9, no. 11, pp. 3543–3553, Nov. 2010.
[2] I. Ahmed, A. Ikhlef, R. Schober, and R. Mallik, "Power allocation for conventional and buffer-aided link adaptive relaying systems with energy harvesting nodes," *IEEE Trans. Wireless Commun.*, vol. 13, no. 3, pp. 1182–1195, Mar. 2014.
[3] O. Orhan and E. Erkip, "Throughput maximization for energy harvesting two-hop networks," in *Proc. IEEE ISIT*, Jul. 2013, pp. 1596–1600.
[4] C. Murthy and N. Mehta, "Tutorial on energy harvesting wireless communication systems," in *Proc. Nat. Conf. Commun.*, *Kanpur, India*, Feb. 2014, pp. 1596–1600.
[5] J. Yang and S. Ulukus, "Optimal packet scheduling in an energy harvesting communication system," *IEEE Trans. Commun.*, vol. 60, no. 1, pp. 220–230, Jan. 2012.
[6] K. Tutuncuoglu and A. Yener, "Optimum transmission policies for battery limited energy harvesting nodes," *IEEE Trans. Wireless Commun.*, vol. 11, no. 3, pp. 1180–1189, Mar. 2012.
[7] P. He, L. Zhao, S. Zhou, and Z. Niu, "Recursive waterfilling for wireless links with energy harvesting transmitters," *IEEE Trans. Veh. Technol.*, vol. 63, no. 3, pp. 1232–1241, Mar. 2014.
[8] J. Yang, O. Ozel, and S. Ulukus, "Broadcasting with an energy harvesting rechargeable transmitter," *IEEE Trans. Wireless Commun.*, vol. 11, no. 2, pp. 571–583, Feb. 2012.
[9] C.-C. Kuan, G.-Y. Lin, H.-Y. Wei, and R. Vannithamby, "Reliable multicast and broadcast mechanisms for energy-harvesting devices," *IEEE Trans. Veh. Technol.*, vol. 63, no. 4, pp. 1813–1826, May 2014.
[10] Z. Fang, T. Song, and T. Li, "Energy harvesting for two-way OFDM communications under hostile jamming," *IEEE Signal Process. Lett.*, vol. 22, no. 4, pp. 413–416, Apr. 2015.
[11] K. Tutuncuoglu, B. Varan, and A. Yener, "Optimum transmission policies for energy harvesting two-way relay channels," in *Proc. IEEE ICC*, Jun. 2013, pp. 586–590.
[12] I. Ahmed, A. Ikhlef, D. Ng, and R. Schober, "Optimal resource allocation for energy harvesting two-way relay systems with channel uncertainty," *Proc. IEEE GlobalSIP*, Dec. 2013, pp. 345–348.
[13] N. Roseveare and B. Natarajan, "An alternative perspective on utility maximization in energy-harvesting wireless sensor networks," *IEEE Trans. Veh. Technol.*, vol. 63, no. 1, pp. 344–356, Jan. 2014.
[14] O. Orhan and E. Erkip, "Optimal transmission policies for energy harvesting two-hop networks," in *Proc. 46th Annu. Conf. CISS*, Mar. 2012, pp. 1–6.
[15] A. Wachter and L. T. Biegler, "On the implementation of an interior-point filter line-search algorithm for large-scale nonlinear programming," *Math. Programm.*, vol. 106, no. 1, pp. 25–57, Mar. 2006.
[16] S. Boyd and L. Vandenberghe, *Convex Optimization*. New York, NY, USA: Cambridge Univ. Press, 2004.

AUTHOR QUERIES

AUTHOR PLEASE ANSWER ALL QUERIES

AQ1 = Please provide keywords.
AQ2 = Table 1 was cited and captured as text. Please check.

END OF ALL QUERIES

Correspondence

Throughput Maximization for a Buffer-Aided Successive Relaying Network Employing Energy Harvesting

Shruti Gupta, Rong Zhang, and Lajos Hanzo

***Abstract*—Energy harvesting (EH)-assisted nodes are capable of significantly prolonging the lifetime of future wireless networks, provided that they rely on appropriate transmission policies, which accommodate the associated stochastic energy arrival. In this paper, a successive-relaying-based network using rechargeable source and relay nodes having limited buffers for both their energy and data storage is considered. The maximization of the network throughput with noncausal knowledge of energy arrivals by the deadline T is formulated as a nonconvex optimization problem, and it is solved using the interior-point optimization (IPOPT) method. The performance of the low-complexity suboptimal scheme was found to reach its maximum when the two phases of the successive relaying protocol have equal duration. The optimal and suboptimal schemes are capable of achieving up to 92% and 88% of the throughput performance of the benchmark scheme. The suboptimal scheme's throughput performance is consistently about 90% of that of the optimal scheme. For asymmetric data (or energy) buffer sizes, it was found that the throughput performance depends on the total (i.e., collective) data (or energy) buffer capacity available in the network and not just on the smallest data buffer.**

***Index Terms*—Author, please supply index terms/keywords for your paper. To download the IEEE Taxonomy go to http://www.ieee.org/ documents/taxonomy_v101.pdf.**

AQ1

I. INTRODUCTION

Cooperative communication is capable of attaining significant throughput and reliability improvements, where the source node (SN) and cooperating relay nodes (RN) expend their energy while processing and transmitting the signal to the destination node (DN). The nodes are typically powered through precharged batteries, but once these batteries are drained, the nodes become dysfunctional [1], [2]. An emerging solution to this vexed problem is the use of energy harvesting (EH) [1]–[3], which has to be capable of accommodating the random arrivals of energy and its storage at the nodes [4].

Hence, EH communication systems have been studied under different network models. In [5]–[7], a single-user EH system was characterized, where beneficial power-allocation strategies were designed under the corresponding EH constraints. This was further extended to the design of an EH-aided broadcast channel in [8] and [9] and to two-way orthogonal frequency-division multiplexing communications [10]. In [8], Yang *et al.* defined the *cutoff power* levels for each user to allocate the optimal power to them, whereas in [9], Kuan *et al.* analyzed the tradeoff between the achievable reliability and throughput for broadcast transmissions relying on erasure codes for EH sensors. In [10], the receiver is designed both for simultaneously processing information and for harvesting energy from the received desired signal, as well as jamming interference a through power splitter. In recent years, cooperative networks have also been studied in the context of EH at the RNs and/or the SN [1]–[3], [11]–[13]. Specifically, in [1], Medepally and Mehta investigated the benefits of relay selection relying on multiple EH amplify-and-forward RNs, whenever they have sufficient energy for transmission. By contrast, in [2], information-buffer-aided link activation was used, which was controlled both by the quality of the links and by the amount of energy buffered at these nodes. Two-hop networks relying either on a single or on a pair of parallel RNs using a successive relaying protocol were investigated to quantify the benefits of both multiple relays and of EH on the average throughput of the system in [3]. In [11], the authors derived the optimal achievable rates for an EH system in the context of two-way relaying employing different relaying strategies. Furthermore, a similar two-way EH relay system employing time-division broadcasting and multiple access broadcasting, which was subjected to channel state uncertainty, was considered in the context of joint energy and transmit time allocation in [12]. Utilizing the structure of a specific problem and the generalized optimality principle, in [13], a new algorithm for constrained utility maximization problems encountered in a cooperative network of wireless sensor nodes is formulated.

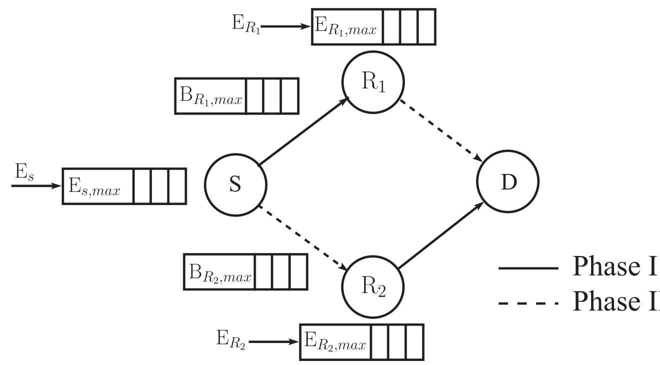

Fig. 1. Successive relaying network where EH nodes are equipped with finite buffer for both energy and data storage.

Against this background, we consider a successive relaying model, which is capable of mimicking a full-duplex (FD) RN, despite relying on a pair of half-duplex (HD) RNs, which are activated alternately in their transmitter and receiver modes to create a virtual FD relay. This HD regime reduces the complexity of the FD system, since the FD RN would require high-complexity interference cancellation at the receiver. In contrast to [3], our model relies on the realistic constraint that EH nodes (SN, RN_1, RN_2) have a finite energy storage capacity and that the RNs also have limited data buffers for storing the source data. We first formulate an optimization problem for the throughput maximization of our successive-relaying-aided network in Fig. 1 having finite buffers, as well as relying on the idealized noncausal knowledge of the energy arrivals at all EH nodes. Then, using the interior-point optimization method (IPOPT), the optimization problem is solved for both optimal and suboptimal schemes, and finally, we quantify the effect of buffer sizes on the throughput of the network based on both schemes. While proof-of-concept studies are indeed

Manuscript received January 28, 2015; revised June 3, 2015 and July 30, 2015; accepted September 8, 2015. This work was supported by the European Research Council under the Advanced Fellow Grant. The review of this paper was coordinated by Dr. L. Zhao.

The authors are with the School of Electronics and Computer Science, University of Southampton, Southampton SO17 1BJ, U.K. (e-mail: sg7g12@ecs.soton.ac.uk; rz@ecs.soton.ac.uk; lh@ecs.soton.ac.uk).

Color versions of one or more of the figures in this paper are available online at http://ieeexplore.ieee.org.

Digital Object Identifier 10.1109/TVT.2015.2477808

valuable, the ultimate purpose of most engineering studies is to attempt a real-world implementation of the proposed techniques. Through this study, we aimed to take the valuable proposals in [3] a step closer to its real-world deployment. Explicitly, the novelty of this contribution is given as follows: 1) We define a practical successive relaying model constrained by both limited energy and data storage buffers at the EH nodes, which dispenses with the idealized simplifying assumption of having infinite buffers [3]; 2) we formulate the optimal transmission policy; and 3) we propose a suboptimal transmission scheme capable of approaching the performance of its optimal counterpart at significantly reduced complexity, which is achieved at the expense of a marginally degraded performance. In our study, we also consider the scenario of asymmetric fading, energy, and data buffers. This paper is organized as follows. In Section II, our system model is presented, which is followed by the formulation of our optimization problem in Section III. Our results are discussed in Section IV, whereas our conclusions are offered in Section V.

II. System Model

We consider the successive relaying technique of [3] having two phases, where the RNs assist the SN's transmission to the DN, as shown in Fig. 1. In Phase I in Fig. 1, the SN transmits to RN_1, whereas RN_2 simultaneously transmits to the DN. By contrast, in Phase II in Fig. 1, SN and RN_1 transmit simultaneously both to RN_2 and to DN, respectively. Thus, the SN is always transmitting, whereas the DN is always receiving during the process. It is assumed that there is no direct link between $SN{-}DN$ and $RN_1{-}RN_2$, as well as that these are decode-and-forward (DF) HD RNs that are located sufficiently far apart from each other to avoid any interference. We assume that SN, RN_1, and RN_2 harvest energy from the environment and have finite energy buffers that can store a maximum of $E_{S,\max}$, $E_{R1,\max}$, and $E_{R2,\max}$ units, respectively, whereas RN_1 and RN_2 are also equipped with data buffers of $B_{R1,\max}$ and $B_{R2,\max}$ packets, respectively. For ease of exposition, we merge the energy arrival events at all the EH nodes into a single time series $(t_0, t_1, \ldots, t_K)$ by considering zero amount of energy arrivals at the nodes that do not harvest energy at some instant t_k. More explicitly, the EH processes at the EH nodes are independent of each other. In other words, the energy arrival instances of a node may be different from those of the other nodes. For example, assume that an energy arrival occurred at node RN_1 at some instant t_k, whereas there was no energy arrival at the other nodes (S and RN_2) at the time instant t_k. In our mathematical analysis, we assumed that at time instant t_k, nodes S and RN_2 harvested zero amount of energy. We set $t_0 = 0$ and $t_K = T$. We represent the amount of energy harvested at SN, RN_1, and RN_2 at time instant t_k as $E_{S,k}$, $E_{R1,k}$, and $E_{R2,k}$ units, respectively, for $k = 0, 1, \ldots K-1$. The time interval between the two consecutive energy arrivals is termed as an *epoch*, whose length is defined as $\tau_k = t_k - t_{k-1}$. The complex-valued channel gains are considered to be constant throughout the communication process preceding the deadline. The channel gain between the nodes L and M is denoted by H_{LM}, where we have $L \in \{SN, R_1N, R_2N\}$ and $M \in \{RN_1, RN_2, DN\}$.

We consider the throughput maximization problem under the idealized simplifying assumption of having prior knowledge about the energy arrivals at all the EH nodes before the commencement of the communication process. We assume that the energy expended at the nodes is only the transmission energy and that perfect "capacity-achieving" codes are used, which facilitate operation exactly at the Shannon capacity, thus determining the rate versus power relationship of a given link, which is given by

$$r\left[p(t)\right] = \log_2\left[1 + Hp(t)\right] \quad (1)$$

where H is the channel gain of the link, and $p(t)$ is the transmission power of the node at time t. As a result of energy arrivals over time and as a benefit of the energy storage capacity at the nodes, any feasible transmission policy should satisfy following constraints.

1) Energy causality constraint: The total energy expended by a node during its transmission session should not exceed the total energy harvested by that node until that time.
2) Energy overflow constraint: The energy exceeding the storage capacity of the energy buffer at the node is lost owing to overflow.
3) Data causality constraint: The total data transmitted by a node during the process should not exceed the total data received by that node until that time.
4) Data overflow constraint: The amount of data exceeding the storage capacity of data buffer is lost due to overflow.

III. Problem Formulation

Here, we first stipulate some properties of the optimal transmission policy in the following two lemmas, which will be used to formulate the throughput maximization problem for the system in Fig. 1. The proof of these lemmas is provided in Appendixes A and B.

Lemma 1: The transmission rate/power of a node is constant between two consecutive energy arrivals but potentially changes when new energy arrives at the node [3].

Lemma 2: The feasible transmission policy ensures that the relays are always on without decreasing the throughput of the system [3].

Based on Lemmas 1 and 2, we can characterize the optimal policy in the following way. There is a constant transmission rate for the pair of nodes between consecutive energy arrivals according to the optimal policy, as formulated in Lemma 1. Therefore, we assume that the transmission power of SN during Phases I and II in Fig. 1 in an epoch is constant and given by $p_{SI,k}$ and $p_{SII,k}$, respectively. Similarly, the transmission power of RN_1 and RN_2 is denoted by $p_{R_1,k}$ and $p_{R_2,k}$, respectively. Lemma 2 implies that we restrict our attention to the specific transmission policies, where both RN_1 and RN_2 are always on for the sake of defining a feasible transmission policy. Thus, we assume that the total transmission time between $SN{-}RN_1$ and $RN_2{-}DN$ is the same and denote this duration of Phase I between the time instants t_{k-1} and t_k by $L_{I,k}$. Similarly, we assume the same transmission time between $SN{-}RN_2$ and $RN_1{-}DN$ in Phase II, which is denoted by $L_{II,k}$, $k = 1, 2, \ldots, K$. Finally, we identify the optimal transmission policy that defines which particular node transmits and when, along with the specific power allocation of each node. We then define a suboptimal scheme, where the duration of each phase of successive relaying is fixed to a particular ratio.

A. Optimal Transmission Policy

Let us now define the optimization problem of maximizing the system throughput by the deadline T. Since RN_2 initially has no data in Phase I in Fig. 1, it is assumed without loss of generality that it starts transmission by delivering $\epsilon > 0$ amount of dummy information to DN, where ϵ is sufficiently small to be ignored for our throughput optimization problem. Upon scheduling the two phases in succession, it is ensured that there is no further throughput loss for the system. In other words, at the beginning of transmission, RN_2 possesses no data from S that can be transmitted to DN; hence, it commences its transmission with ϵ dummy packets. However, subsequently, the transmission phases occur in immediate succession without any interval. This ensures that there is no need to send dummy packets, and thus, no further loss of system throughput is imposed. Similar assumptions were also made in [3]. We first define the throughput of the nodes in different phases based on the rate versus power relationship (1) mentioned in Section II as

$$\alpha_{R1,k} = L_{II,k}\log_2(1+H_{R1D}p_{R1,k})$$
$$\alpha_{R2,k} = L_{I,k}\log_2(1+H_{R2D}p_{R2,k}) \tag{2a}$$
$$\alpha_{SI,k} = L_{I,k}\log_2(1+H_{SR1}p_{SI,k})$$
$$\alpha_{SII,k} = L_{II,k}\log_2(1+H_{SR2}p_{SII,k}). \tag{2b}$$

Now, the optimization problem is defined over $L_{I,k}$, $L_{II,k}$, $\alpha_{SI,k}$, $\alpha_{SII,k}$, $\alpha_{R1,k}$, and $\alpha_{R2,k}$, (3a)–(3m), shown at the bottom of the page.

Note that when (3h)–(3i) are evaluated at $k=K$, the total amount of data delivered to DN is equal to the amount of data transferred by RN_1 and RN_2; hence, the throughput maximization problem corresponds to the maximization of the amount of data transmitted by both the RNs, as formulated in (3a). The problem in (3) is a non-convex optimization problem, owing to the nonconvex energy storage constraints defined in (3e)–(3g), which can be efficiently solved using the IPOPT method, as given in Appendix C.

B. Suboptimal (Alternate) Transmission Policy

In this scheme, we set the duration of Phase I in Fig. 1 to be equal to $\eta\%$; of the length of an epoch, i.e., we have

$$L_{I,k} = \frac{\eta}{100}\tau_k, \quad L_{II,k} = \tau_k - \frac{\eta}{100}\tau_k. \tag{4}$$

$$\text{maximize} \quad \sum_{k=1}^{K} \alpha_{R1,k} + \alpha_{R2,k} \tag{3a}$$

subject to

Energy causality constraints (constraint 1 in Section II) at SN, RN_1, and RN_2:

$$\sum_{j=1}^{k} \frac{L_{I,j}}{H_{SR1}}\left(2^{\left(\frac{\alpha_{SI,j}}{L_{I,j}}\right)}-1\right) + \frac{L_{II,j}}{H_{SR2}}\left(2^{\left(\frac{\alpha_{SII,j}}{L_{II,j}}\right)}-1\right) \le \sum_{j=0}^{k-1} E_{S,j} \qquad \forall\, k \tag{3b}$$

$$\sum_{j=1}^{k} \frac{L_{II,j}}{H_{R1D}}\left(2^{\left(\frac{\alpha_{R1,j}}{L_{II,j}}\right)}-1\right) \le \sum_{j=0}^{k-1} E_{R1,j} \qquad \forall\, k \tag{3c}$$

$$\sum_{j=1}^{k} \frac{L_{I,j}}{H_{R2D}}\left(2^{\left(\frac{\alpha_{R2,j}}{L_{I,j}}\right)}-1\right) \le \sum_{j=0}^{k-1} E_{R2,j} \qquad \forall\, k. \tag{3d}$$

Energy overflow constraints (constraint 2 in Section II) at SN, RN_1, and RN_2:

$$\sum_{j=0}^{k} E_{S,j} - \sum_{j=1}^{k} \frac{L_{I,j}}{H_{SR1}}\left(2^{\left(\frac{\alpha_{SI,j}}{L_{I,j}}\right)}-1\right) + \frac{L_{II,j}}{H_{SR2}}\left(2^{\left(\frac{\alpha_{SII,j}}{L_{II,j}}\right)}-1\right) \le E_{S,\max} \qquad \forall\, k \tag{3e}$$

$$\sum_{j=0}^{k} E_{R1,j} - \sum_{j=1}^{k} \frac{L_{II,j}}{H_{R1D}}\left(2^{\left(\frac{\alpha_{R1,j}}{L_{II,j}}\right)}-1\right) \le E_{R1,\max} \qquad \forall\, k \tag{3f}$$

$$\sum_{j=0}^{k} E_{R2,j} - \sum_{j=1}^{k} \frac{L_{I,j}}{H_{R2D}}\left(2^{\left(\frac{\alpha_{R2,j}}{L_{I,j}}\right)^{i}}-1\right) \le E_{R2,\max} \qquad \forall\, k. \tag{3g}$$

Data causality constraints (constraint 3 in Section II) at RN_1 and RN_2:

$$\sum_{j=1}^{k} \alpha_{R1,j} \le \sum_{j=1}^{k} \alpha_{SI,j} \qquad \forall\, k \tag{3h}$$

$$\sum_{j=1}^{k} \alpha_{R2,j} \le \sum_{j=1}^{k} \alpha_{SII,j} \qquad \forall\, k. \tag{3i}$$

Data overflow constraints (constraint 4 in Section II) at RN_1 and RN_2:

$$\sum_{j=1}^{k} \alpha_{SI,j} - \sum_{j=1}^{k-1} \alpha_{R1,j} \le B_{R1,\max} \qquad \forall\, k \tag{3j}$$

$$\sum_{j=1}^{k} \alpha_{SII,j} - \sum_{j=1}^{k-1} \alpha_{R2,j} \le B_{R2,\max} \qquad \forall\, k. \tag{3k}$$

Half duplex constraint due to the HD relays RN_1 and RN_2:

$$L_{I,k} + L_{II,k} \le \tau_k \qquad \forall\, k. \tag{3l}$$

Feasibility constraints at SN, RN_1 and RN_2:

$$\alpha_{SI,k} \ge 0, \quad \alpha_{SII,k} \ge 0, \quad \alpha_{R1,k} \ge 0; \alpha_{R2,k} \ge 0, \quad L_{I,k} \ge 0, \quad L_{II,k} \ge 0 \qquad \forall\, k \tag{3m}$$

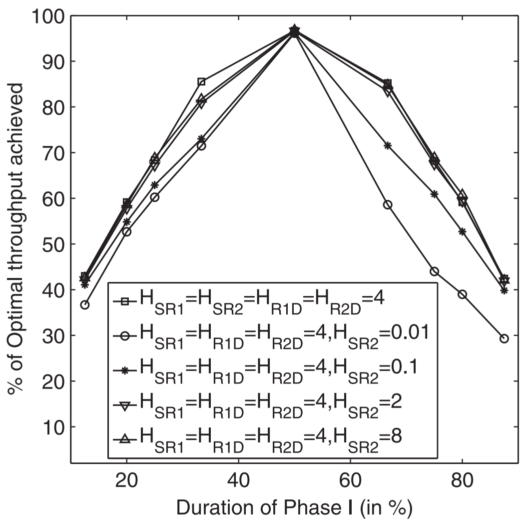

Fig. 2. Relation between percentage of optimal throughput achieved for varying duration of Phase I occurring in an EH epoch with sufficient energy and data buffer sizes (5 and 2, respectively) for different settings of channel gains.

Using (4), the optimization problem is relaxed for this suboptimal scheme and can be reformulated by omitting (3l) from (3). This is again a nonconvex optimization problem; hence, it may be solved using the IPOPT method. This scheme is termed suboptimal, since the duration of the phases has been deliberately fixed for the sake of reducing the complexity[1] of the optimization problem.

IV. Performance Results

Here, we evaluate the performance of the proposed buffer-aided successive relaying system relying on offline power allocation in terms of the optimal throughput achieved by the deadline of $T = 10$ s. We assume that the EH process of both the SN and the RNs independently takes values from $[0, E_{\max} = 5]$ units, where the energy is uniformly distributed under an exponential inter-arrival time at a rate of $\lambda_e = 5$ units/s. The deterministic channel gains are set to the values $H_{SR1} = H_{SR2} = H_{R1D} = H_{R2D} = 4$, except otherwise mentioned. Our results quantify the throughput of the system as a function of both data and energy buffer capacity for both optimal and suboptimal schemes that are benchmarked against the infinite-storage-based optimal scheme defined in [3]. Our benchmark scheme of [3] is insensitive to the buffer sizes, since it considers infinite storage capacities at all the EH nodes for both energy and data, thereby providing an upper bound to our proposed system.

The percentage duration of Phases I and II in Fig. 1 is not fixed for the optimal scheme, whereas they have been fixed to a specific ratio for the suboptimal scheme for the sake of complexity reduction. Hence, our first goal was to identify the specific ratio of the durations of Phases I and II that would maximize the throughput of the suboptimal scheme. Fig. 2 shows the specific percentage of the optimal throughput, which was actually achieved by varying the proportion of the Phase I duration (L_I) in each of the EH epochs, along with the symmetric $(H_{SR1} = H_{SR2} = H_{R1D} = H_{R2D} = 4)$ and asymmetric settings of the channel fading gain for $SN{-}RN_2$. The performance of the suboptimal scheme peaks when the durations of both phases are equal. For the other scenarios, the throughput is lower, because the amount of data transmitted between SN and DN is limited by the shorter phase. It is shown in Fig. 2 that, as the duration of the shorter phase increases, the throughput also increases. It is interesting to note

[1]The complexity analysis of both schemes is beyond the scope of this paper.

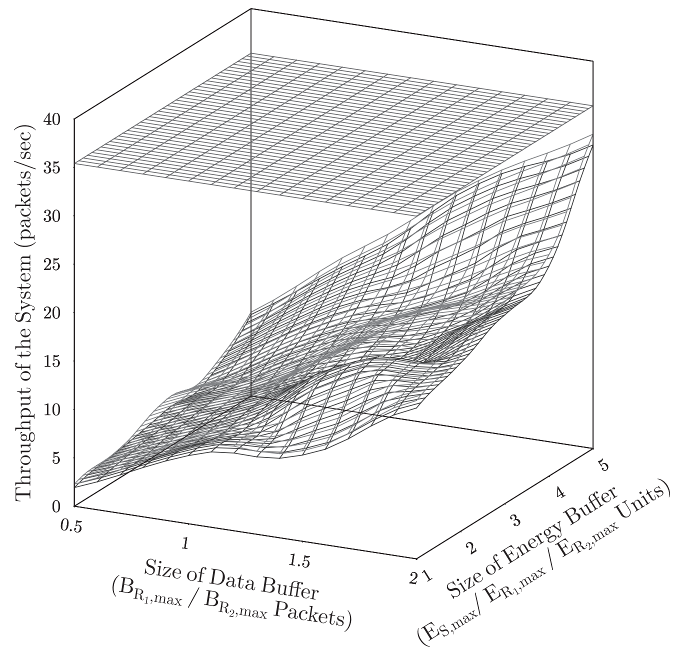

Fig. 3. Impact of the energy and data buffer sizes at all the EH nodes on the throughput of the system by the deadline T. The constant green surface represents the throughput of the benchmark scheme [3], whereas the pink and blue surfaces depict our optimal and suboptimal transmission policies, respectively.

that in the scenarios of very low channel gain, i.e., for $H_{SR2} = 0.01$ and $H_{SR2} = 0.1$, there exists asymmetry in the throughput achieved by the system. The reason behind this trend is that when the duration of Phase I is higher than that of Phase II, the channel gain of path $SN{-}RN_2$ limits the amount of data that can be otherwise transmitted to RN_2. As shown in Fig. 2, when the duration of Phase I is 50% of the EH epoch, the suboptimal scheme achieves approximately 97% of the optimal scheme's throughput. Hence, in the following discussions, we consider a suboptimal scheme, where the duration of each phase is 50% of the epoch duration.

The 3-D characterization of the system in Fig. 1 is provided in Fig. 3. Specifically, Fig. 3 shows the overall throughput of the system as a function of the size of both energy and data buffers at the EH nodes. It can be clearly observed that, with the increase in the size of buffers at the EH nodes, the throughput of our proposed schemes improve owing to increased availability of energy and data storage capacity at the EH nodes, supporting a larger amount of data transmission to DN. However, the throughput of the benchmark scheme [3] is constant, i.e., independent of the buffer sizes, as it relies on the idealized settings where EH nodes possess infinite energy and data storage capacity. Moreover, our optimal scheme performs only marginally better than our less complex suboptimal scheme, because the duration of each phase is fixed in the suboptimal scheme. This would, in turn, result in limiting the amount of data that can be transmitted to DN during successive relaying phases. To closely analyze the impact of the energy and data buffer capacities at the EH nodes on the overall system throughput, we present the 2-D curves corresponding to the individual analysis of the energy buffer size while keeping the data buffer size constant, and *vice versa*.

The results in Fig. 4 show the throughput of the system against the size of the battery in the presence of sufficient, insufficient, and asymmetric data buffer sizes for both optimal and suboptimal schemes. As expected, upon increasing the battery size, the throughput of the system is improved, owing to the availability of increased amount of

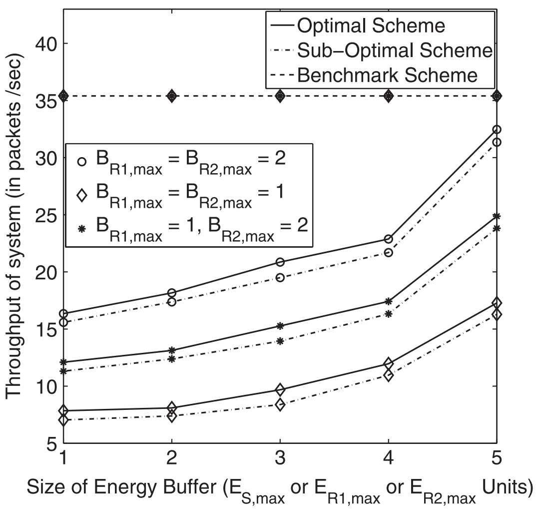

Fig. 4. Impact of energy buffer size at all the EH nodes with sufficient (two packets), insufficient (one packet), and asymmetric data buffer capacity at the RNs on the throughput of the system by the deadline T.

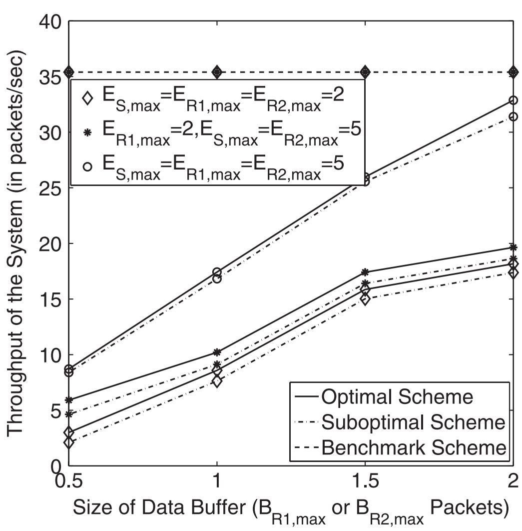

Fig. 5. Impact of data buffer size at the RNs with sufficient (five units), insufficient (two units), and asymmetric battery capacities at EH nodes over throughput of the system by the deadline T.

energy (due to the increase in buffer size) for transmission. Moreover, it can be observed that for sufficient (or insufficient) data storage, our optimal system is capable of achieving 92% (or 50%) of the benchmark scheme's throughput performance [3], whereas our suboptimal scheme performs slightly worse than the optimal scheme, reaching 88% (or 46%) of the benchmark system's throughput value in [3], when the battery capacity of the EH nodes is sufficiently high ($E_{S,\max} = E_{R_1,\max} = E_{R_2,\max} = 5\,\text{units}$). Furthermore, for asymmetric settings having unequal data buffers at RN_1 and RN_2, the throughput becomes lower than that for sufficiently large storage, since RN_1 is now acting as a bottleneck, preventing the flow of data to DN. On the other hand, for this asymmetric setting, the throughput becomes higher than that for insufficient storage, since the node RN_2 has a higher data storage capacity, thereby supporting a higher data rate to DN. The suboptimal scheme's throughput performance was 95.2%, 90.7%, and 93.7% of that of the optimal scheme for the scenarios of sufficient, insufficient, and asymmetric data buffers, respectively.

Similarly, Fig. 5 shows the throughput of the system as a function of the data buffer size at the RNs with sufficient, insufficient, and asymmetric energy buffer sizes for both optimal and suboptimal schemes. It is clearly demonstrated that as the size of the data buffer increases, the amount of data successfully transmitted to the DN also increases for both schemes, indicating that the optimal and suboptimal schemes have quite similar performance. The reason behind this trend is the reduction of overflowing data buffers owing to the larger capacities of these buffers at the RNs. Furthermore, for sufficient (or insufficient) battery capacities, our optimal system having finite buffers is capable of achieving 92% (or 52%) of the throughput compared with our suboptimal scheme that performs comparably, since it achieves 88% (or 49%) of the benchmark system's throughput [3] for the maximum data buffer size of $B_{R_1,\max} = B_{R_2,\max} = 2$ packets. Furthermore, for asymmetric settings having unequal energy buffers at RN_1 and RN_2, the throughput becomes lower than that for a sufficiently large storage, since RN_1 is low on energy, hence preventing the flow of data to DN. On the other hand, for this asymmetric setting, the throughput becomes higher than that for insufficient storage, since the node RN_2 has a higher energy storage capacity, consequently supporting a higher data rate to DN. Moreover, the suboptimal scheme achieves 96.7%, 87.3%, and 94.2% of the throughput of our optimal scheme for sufficient, insufficient, and asymmetric energy buffers, respectively.

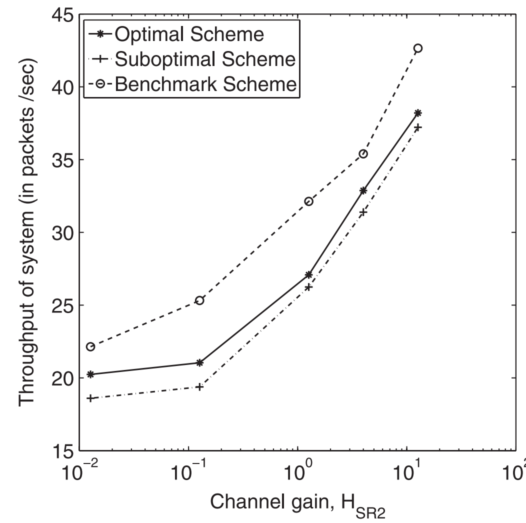

Fig. 6. Impact of asymmetric fading from S to RN_2 for sufficient battery and data buffer capacities (five units and two packets, respectively) at EH nodes on throughput of the system by the deadline T.

Fig. 6 shows the throughput of the system as a function of the asymmetric channel gain of the $SN - RN_2$ path (H_{SR2}) for the scenario of having a sufficiently high data and energy buffer size at the EH nodes, where all other channel gains are set to $H_{SR1} = H_{R1D} = H_{R2D} = 4$. It can be clearly seen that as the channel gain H_{SR2} increases, the throughput of the system increases for all the schemes owing to the rate–power relationship mentioned in (1). This means that as the value of the channel gain increases, the amount of data transmitted from SN to RN_2 increases, and so does the amount of data reaching the DN, hence, also increasing the overall throughput of the system. As expected, the benchmark scheme represents the upper bound of the system's throughput for an asymmetric setting of the channel gain, as it relies on the idealized assumptions of infinite data and energy storage capacities at the EH nodes. However, our optimal scheme performs better than the suboptimal scheme owing to the fixed duration of phases in the successive relaying protocol of the latter scheme.

In Fig. 7, we considered the throughput of the system as a function of the data buffer capacity at the RNs for the scenario of asymmetric channel gains and asymmetric energy buffer capacity. Explicitly, we

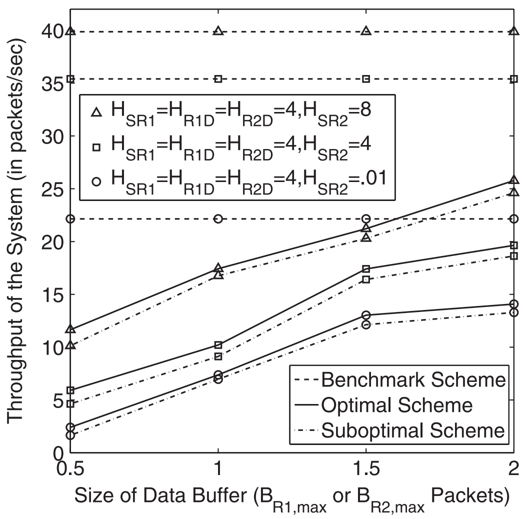

Fig. 7. Impact of data buffer size at the RNs with asymmetric channel gains and battery capacities ($E_{S,\max} = E_{R2,\max} = 5$ units, and $E_{R1,\max} = 2$ units) at EH nodes over throughput of the system by the deadline T.

have used $E_{S,\max} = E_{R2,\max} = 5$ units and $E_{R1,\max} = 2$ units at the EH nodes. The benchmark scheme provides an upper bound for our proposed schemes and has a constant throughput, since it is unaffected by the data and energy buffer capacity at the EH nodes. Interestingly, the throughput of the system improves upon increasing the value of the channel gains, which becomes explicit by observing the rate–power relationship of (1). Moreover, the asymmetric setting of energy buffers at the EH nodes of the proposed scheme results in limiting the throughput achieved by the system, because RN_1 is acting as the bottleneck owing to the low energy buffer capacity.

In light of the preceding study, our findings for the realistic simulation parameters in Table I may be summarized as follows. AQ2

1) The performance of the suboptimal scheme as a percentage of the throughput achieved by the optimal scheme reaches its maximum when the two phases of the successive relaying protocol have equal duration.
2) The optimal and suboptimal schemes are capable of achieving up to 92% and 88% of the benchmark scheme's throughput [3] for sufficiently high energy and data buffer capacities.
3) The suboptimal scheme's throughput is consistently about 90% of that of the optimal scheme.
4) For asymmetric data (or energy) buffer sizes, the attainable throughput depends on the total (i.e., collective) data (or energy) buffer capacity available in the network and not only on the smallest data buffer.

V. Conclusion

In this paper, we have considered the throughput optimization of an EH-assisted two-hop network using a buffer-aided successive relaying protocol. Under the assumption of known energy arrivals, we defined the related nonconvex optimization problem and proposed both optimal and suboptimal schemes to maximize the data delivered to the DN by the deadline. Then, using the *interior-point* method, an efficient solution was found for both schemes. Finally, our results justify that both our optimal and suboptimal schemes are capable of performing close to the benchmark system [3]. Furthermore, the less-complex suboptimal scheme is capable of approaching the performance of our optimal scheme at the expense of a slight performance degradation, provided that the EH nodes are equipped with sufficiently large buffers for both energy and data storage. Our future work may consider EH-aided adaptive transceiver schemes.

Appendix A
Proof of Lemma 1

This proof is an extension of that derived for the point-to-point case in [5] to the two-hop scenario defined in this paper. Let us assume that the transmitter nodes (SN, RN_1, RN_2) change their transmission rate between two EH instances t_i and t_{i+1}. Let us furthermore denote the rates by $r_{M,n}$ and $r_{M,n+1}$ and the instant when the rate changes by t'_i, where we have $M \in \{SI, R2\}$ in Phase I and $M \in \{SII, R1\}$ in Phase II of the successive relaying protocol. Correspondingly, the duration of each phase can be written as $L_{I,n}$, $L_{I,n+1}$, $L_{II,n}$, and $L_{II,n+1}$. Let us now consider the duration $[t_i, t_{i+1})$. The total energy consumed in this duration at SN is $p_{SI,n}L_{I,n} + p_{SII,n}L_{II,n} + p_{SI,n+1}L_{I,n+1} + p_{SII,n+1}L_{II,n+1}$. Similarly, the total energy consumed at RN_1 is $p_{R1,n}L_{II,n} + p_{R1,n+1}L_{II,n+1}$ and that at RN_2 is $p_{R2,n}L_{I,n} + p_{R2,n+1}L_{I,n+1}$. Let us now consider SN in more detail and define

$$
\begin{aligned}
p'_{SI} &= \frac{p_{SI,n}L_{I,n} + p_{SI,n+1}L_{I,n+1}}{t_{i+1} - t_i} \\
p'_{SII} &= \frac{p_{SII,n}L_{II,n} + p_{SII,n+1}L_{II,n+1}}{t_{i+1} - t_i} \\
r'_{SI} &= r\left[p'_{SI}\right] = r\left[\frac{p_{SI,n}L_{I,n} + p_{SI,n+1}L_{I,n+1}}{t_{i+1} - t_i}\right] \\
r'_{SII} &= r\left[p'_{SII}\right] = r\left[\frac{p_{SII,n}L_{II,n} + p_{SII,n+1}L_{II,n+1}}{t_{i+1} - t_i}\right].
\end{aligned}
$$

Let us now use these r'_{SI} and r'_{SII} as the new transmission rates for Phases I and II at SN over $[t_i, t_{i+1})$ and keep the rest of the rates the same as in the original policy. It is easy to observe that the new transmission policy is feasible, since all the energy constraints are satisfied under this policy. On the other hand, we can write the total number of packets that are departed from SN in both of the phases over this duration under this new policy as

$$
\begin{aligned}
&(r'_{SI} + r'_{SII})(t_{i+1} - t_i) = (r\left[p'_{SI}\right] + r[p'_{SII}])(t_{i+1} - t_i) \\
&\quad = \left(r\left[\frac{p_{SI,n}L_{I,n} + p_{SI,n+1}L_{I,n+1}}{t_{i+1} - t_i}\right]\right)(t_{i+1} - t_i) \\
&\qquad + \left(r\left[\frac{p_{SII,n}L_{II,n} + p_{SII,n+1}L_{II,n+1}}{t_{i+1} - t_i}\right]\right)(t_{i+1} - t_i) \quad \text{(5a)} \\
&\quad \geq (r[p_{SI,n}]L_{I,n} + r[p_{SI,n+1}]L_{I,n+1}) \\
&\qquad + (r[p_{SII,n}]L_{II,n} + r[p_{SII,n+1}]L_{II,n+1}) \quad \text{(5b)} \\
&\quad = r_{SI,n}L_{I,n} + r_{SI,n+1}L_{I,n+1} + r_{SII,n}L_{II,n} \\
&\qquad + r_{SII,n+1}L_{II,n+1} \quad \text{(5c)}
\end{aligned}
$$

where the inequality in (5b) follows from (1) in Section II, which is a concave function of the transmission power p. Therefore, the total number of packets transmitted by SN in this duration under the new policy is higher than those that are departed under the original policy. Similarly, we can prove that the RNs under this new policy will send more data to DN. If we keep all the rates constant, the transmissions will deliver larger amounts of data to DN by the deadline. This contradicts the optimality of the original transmission policy.

APPENDIX B
PROOF OF LEMMA 2

The proof derived for the two-relay case extends the single-relay case of [14]. In the case of two parallel relays, we consider a feasible transmission policy where one of the relays (e.g., RN_1) is not always on, i.e., it is not transmitting or receiving data all the time. Now, if we have an idle time interval right at the beginning of Phase I, we can extend the epoch of SN in Phase II, ensuring that there is no idle time. Note that this strategy continues to satisfy all the causality and storage constraints. On the other hand, if an idle time duration occurs at the beginning of Phase II, we can delay the epoch of relay RN_1 without violating the feasibility of our policy, because it can store more energy in the meantime, and the previous argument can be used to extend the epoch of RN_2 during Phase I to avoid any idle time. Similarly, we can consider the scenario when RN_2 is not always on. Therefore, we remove the idle times by increasing the transmission duration of one of the nodes (SN or RNs) while keeping the total amount of transmitted data the same. Since the rate–power relation of (1) is concave, the new policy conveys the same amount of data to DN while consuming less energy. Hence, it is feasible. Moreover, using this proof, we can say that there exists an optimal policy, where SN and DN are always on for the twin-relay system relying on a successive relaying protocol.

APPENDIX C
INTERIOR-POINT OPTIMIZATION METHOD

The relevant optimization techniques include IPOPT, LOQO, and KNITRO [15]. The IPOPT method is more efficient than the other two techniques, because it relies on tighter termination bounds and utilizes comparable CPU time to evaluate a higher number of objective function values and iterations [15]. The IPOPT method involves the primal–dual interior-point algorithm with the aid of a so-called filter line-search method invoked for nonlinear programming [15], [16], which improves its robustness over that of LOQO and KNITRO. In the primal–dual interior-point method, both primal and dual variables are updated, whereas primal and dual iterates do not have to be feasible. The search direction in this method is obtained using Newton's method applied to the modified Karush–Kuhn–Tucker equations. However, the basic idea behind the filter line-search algorithm involves considering a trial point during the backtracking line search, where this trial point is considered to be acceptable if it leads to sufficient progress toward achieving the optimization goal. This algorithm maintains a "filter," which is a set of values that both the objective function and the constraint violation functions are prohibited from returning. For a trial point to be successful, the values of the objective function and the constraint violation functions evaluated at that trial point should not be a member of the filter. This filter is updated at every iteration to ensure that the algorithm does not cycle in the neighborhood of the previous iterate [15].

REFERENCES

[1] B. Medepally and N. Mehta, "Voluntary energy harvesting relays and selection in cooperative wireless networks," *IEEE Trans. Wireless Commun.*, vol. 9, no. 11, pp. 3543–3553, Nov. 2010.

[2] I. Ahmed, A. Ikhlef, R. Schober, and R. Mallik, "Power allocation for conventional and buffer-aided link adaptive relaying systems with energy harvesting nodes," *IEEE Trans. Wireless Commun.*, vol. 13, no. 3, pp. 1182–1195, Mar. 2014.

[3] O. Orhan and E. Erkip, "Throughput maximization for energy harvesting two-hop networks," in *Proc. IEEE ISIT*, Jul. 2013, pp. 1596–1600.

[4] C. Murthy and N. Mehta, "Tutorial on energy harvesting wireless communication systems," in *Proc. Nat. Conf. Commun., Kanpur, India*, Feb. 2014, pp. 1596–1600.

[5] J. Yang and S. Ulukus, "Optimal packet scheduling in an energy harvesting communication system," *IEEE Trans. Commun.*, vol. 60, no. 1, pp. 220–230, Jan. 2012.

[6] K. Tutuncuoglu and A. Yener, "Optimum transmission policies for battery limited energy harvesting nodes," *IEEE Trans. Wireless Commun.*, vol. 11, no. 3, pp. 1180–1189, Mar. 2012.

[7] P. He, L. Zhao, S. Zhou, and Z. Niu, "Recursive waterfilling for wireless links with energy harvesting transmitters," *IEEE Trans. Veh. Technol.*, vol. 63, no. 3, pp. 1232–1241, Mar. 2014.

[8] J. Yang, O. Ozel, and S. Ulukus, "Broadcasting with an energy harvesting rechargeable transmitter," *IEEE Trans. Wireless Commun.*, vol. 11, no. 2, pp. 571–583, Feb. 2012.

[9] C.-C. Kuan, G.-Y. Lin, H.-Y. Wei, and R. Vannithamby, "Reliable multicast and broadcast mechanisms for energy-harvesting devices," *IEEE Trans. Veh. Technol.*, vol. 63, no. 4, pp. 1813–1826, May 2014.

[10] Z. Fang, T. Song, and T. Li, "Energy harvesting for two-way OFDM communications under hostile jamming," *IEEE Signal Process. Lett.*, vol. 22, no. 4, pp. 413–416, Apr. 2015.

[11] K. Tutuncuoglu, B. Varan, and A. Yener, "Optimum transmission policies for energy harvesting two-way relay channels," in *Proc. IEEE ICC*, Jun. 2013, pp. 586–590.

[12] I. Ahmed, A. Ikhlef, D. Ng, and R. Schober, "Optimal resource allocation for energy harvesting two-way relay systems with channel uncertainty," *Proc. IEEE GlobalSIP*, Dec. 2013, pp. 345–348.

[13] N. Roseveare and B. Natarajan, "An alternative perspective on utility maximization in energy-harvesting wireless sensor networks," *IEEE Trans. Veh. Technol.*, vol. 63, no. 1, pp. 344–356, Jan. 2014.

[14] O. Orhan and E. Erkip, "Optimal transmission policies for energy harvesting two-hop networks," in *Proc. 46th Annu. Conf. CISS*, Mar. 2012, pp. 1–6.

[15] A. Wachter and L. T. Biegler, "On the implementation of an interior-point filter line-search algorithm for large-scale nonlinear programming," *Math. Programm.*, vol. 106, no. 1, pp. 25–57, Mar. 2006.

[16] S. Boyd and L. Vandenberghe, *Convex Optimization*. New York, NY, USA: Cambridge Univ. Press, 2004.

AUTHOR QUERIES

AUTHOR PLEASE ANSWER ALL QUERIES

AQ1 = Please provide keywords.
AQ2 = Table 1 was cited and captured as text. Please check.

END OF ALL QUERIES